Grading and Tissue-Specific Diagnosis

11

A.M. De Schepper

Contents

11.1 Introduction

Characterization consists of both grading and tissue-specific diagnosis.

While tissue specific diagnosis implies pathological typing, grading implies a differentiation between benign and malignant tumors and definition of malignancy grade. Although pathology will always remain the gold standard in the diagnosis of soft tissue tumors, prediction of a specific histologic diagnosis remains one of the ultimate goals of each new imaging technique [34]. Moreover, decisions regarding biopsy and treatment could be simplified if a specific diagnosis or a limited differential diagnosis could be provided on the basis of imaging [1, 36].

Sundaram stressed the importance of "naming" soft tissue masses based on MR imaging criteria, working on the premise that one's inability to "name", or provide a succinct differential diagnosis requires the lesion to be considered "indeterminate" and biopsied. The approach to such indeterminate lesions is that they are sarcomas until microscopically proven otherwise [38].

Benign soft tissue tumors outnumber their malignant counterparts by about 100 to 1. Otherwise most cutaneous and subcutaneous masses are very small and are often excised without imaging studies. As a consequence 60% of the soft tissue tumors in adults who are referred for evaluation by medical imaging are benign, this proportion increasing to 75% in the pediatric age group. The major role of grading consists merely in recognizing benign soft tissue tumors which will be excluded from further invasive diagnostic and therapeutic procedures.

The statement that disease stage and grade are more important than tumor type with respect to five-year survival (American Joint Committee of Soft Tissue Sarcomas) [23] was discussed at the 20th anniversary meeting of the Soft Tissue and Bone Sarcoma Group of the European Organization for Research and Treatment of Cancer (EORTC) in Amsterdam (April 11–13, 1996). There was a broad consensus that staging and grading systems should always be based on tumors of one specific histological type, because conventional staging and grading parameters are of different importance in different tumor types. Also the significance and the predictive value of the various histologic parameters vary in different types of sarcoma. And because of morphologic variations in different portions of the tumor, the grade is determined on the basis of the least differentiated area and its extent [19, 24, 53]. The pathologist's perspective on grading is well described in Chap. 8.

11.2 Grading

Grading refers to differentiation between benign and malignant tumors and definition of malignancy grade. Moreover tumor grading is also an important staging parameter as already discussed. Well known histological grading parameters are cellularity, cellular pleomorphism, mitotic rate, matrix and presence of necrosis. In this regard presence of necrosis, tumor size and most importantly mitotic count are significantly correlated with the duration of survival or the time to distant metastases [48]. Since most of these parameters influence signal intensity on MRI, the grading capacity of this imaging method seemed promising. Nevertheless, there is still much controversy regarding the value of imaging, in particular of MRI in the differentiation of benign and malignant soft tissue tumors [10]. However, although the signal characteristics of both benign and malignant tumors overlap frequently, certain benign lesions, because of a certain contained tissue type or material, a characteristic shape, or a favored location can

Table 11.1. Soft tissue tumor (STT) grading parameters

Origin (subcutaneous, fascial, intramuscular, mixed)
Location
Distribution Intracompartmental Extracompartmental
Size
Shape
Margins
Relationship with superficial fasciae
Neurovascular bundle displacement/encasement
Bone involvement
Signal intensity on different pulse sequences
Signal homogeneity
Changing pattern of homogeneity
Low signal intensity septations
Peritumoral edema
Hemorrhage
Contrast enhancement Static studies (type, intensity) Dynamic studies (ratio, slope)
Diffusion-weighted MRI

be accurately diagnosed on MR imaging. Initially though to be limited to a handful, the list of soft-tissue conditions that can be diagnosed on MR imaging continues to grow. Soft tissue masses that do not demonstrate distinguishing features on MR imaging should be considered indeterminate and will require biopsy [39]. These items will be discussed in depth in the part devoted to characterization in this same chapter.

A variety of imaging-grading parameters have been described in the literature, and are listed in Table 11.1.

11.2.1 Individual Parameters

Examples of commonly used individual parameters for predicting malignancy are *intensity* and *homogeneity of the MR signal* with different pulse sequences. High signal intensity (SI) on T2-WI [40] and inhomogeneity on T1-WI are sensitive parameters but present with an unacceptable low specificity. Because 90% of the malignant lesions are inhomogeneous ("disorganized" or "hectic") absence of heterogeneity is a reliable negative predictive indicator for the presence of malignancy [51]. Otherwise smaller lesions tend to be more homogeneous, whether they are benign or malignant. Concerning signal intensity, high grade malignant soft tissue tumors may present with low to intermediate signal intensity on T2-WI as a consequence of hypercellularity, increased nucleocytoplasmatic index and an altered ratio between cellular and interstitial components both resulting in a decreased amount of intra- and extracellular water [5, 7, 13]. In this regard lymphomas and non differentiated (high grade) sarcomas may present with low SI on T2-weighted images and have to be differentiated from tumors showing recurrent intralesional bleeding and hemosiderin loading causing shortening of the T2-relaxation time and consequently lower SI on T2-WI.

Clear cell sarcomas (deep seated melanomas) may present with increased SI on T1-weighted images, depending on their content on melanin which shortens the T1-relaxation time [12].

Changing homogeneity (from homogeneous on T1-WI to heterogeneous on T2-WI) and the presence of a lobular morphology with intervening low signal intratumoral septations were reported by Hermann respectively with a sensitivity of 72 and 80%, respectively, and a specificity of 87 and 91%, respectively, in predicting malignancy [26].

Galant et al. described a grading system of subcutaneous soft tissue tumors by means of their *relationship with the superficial fascia* on MRI. Obtuse angles between superficial fascia and a subcutaneous mass crossing the fascia indicate a probability of malignancy six to seven times that for lesions that do not cross the fascia or have contact with acute angles. Exceptions are vascular and neurogenic tumors, which can cross the fascia through preexisting anatomical channels and fibromatosis [21].

Location has a limited value in differentiating soft tissue tumors. In contradistinction to malignant tumors, benign ones frequently have a preferential location. In this regard elastofibroma has a predilection for the subscapular region, PVNS for the knee, nodular fasciitis for the forearm, desmoids for the deltoid and gluteal region, glomus tumors for the subungual soft tissues while soft tissue tumors of the hand and wrist are benign in more than 90% of the cases, and intra-articular tumoral lesions being almost always benign. Concerning malignant lesions, soft tissue sarcomas have a predilection for the thigh and in particular synovial cell sarcomas for the foot. In this same regard location can be a valuable parameter in differentiating between low-grade liposarcomas and benign lipomas. Subcutaneous fatty tumors are mostly benign lipomas and if they are of low grade malignancy they never metastasize [51]. The parameter location will be discussed further in the section "characterization" of this chapter.

Although the *size* and *shape* of the lesion at detection seem unlikely to contribute to tumor grading, Tung combined the data from three investigations and postulated that a diameter of less than 3 cm is a reasonable indicator that a lesion is benign, as this threshold is associated with a positive predictive value of 88%. Conversely, a diameter of 5 cm predicts the malignant nature of a soft tissue mass with a sensitivity of 74%, specificity of 59%, and an accuracy of 66% [44].

Although benign tumors tend to be well-delineated and, conversely, malignant tumors have rather ill-defined margins, several studies have concluded that the *margin* (well-defined versus infiltrating) of a soft tissue mass on MRI is of no statistical relevance in predicting of malignancy. Moreover, Bongartz reported that aggressive sarcomas may have a pseudocapsule while benign lesions such as desmoid tumors may invade neighboring tissues [7, 49].

Peritumoral edema, shown on T2-weighted images as an ill-defined area of high signal intensity, can indicate infiltrative tumor, reparative inflammation, or both, and as a consequence is not helpful as a grading parameter [24].

Involvement of adjacent bone, *extracompartmental* distribution, and *encasement of the neurovascular bundle* are relatively uncommon findings that are specific but insensitive signs of malignancy. They are also seen in aggressive benign soft tissue lesions including desmoids, hemangiomas, and pigmented villonodular synovitis. Osseous invasion was studied by Elias et al. [16]. They found that cortical and medullary signal intensity changes and cortical destruction observed on MRI are highly sensitive and highly specific signs of osseous invasion by soft tissue sarcoma. Increasing maximal diameter and increasing circumference of osseous abutment by the tumor did not result in a statistically significant increase in the likelihood of osseous invasion. Moreover their study proved that observation of a completely preserved soft tissue interface on T1-weighted images, even in the presence of peritumoral edema and/or reactive changes extending to the bone surface, has a NPV of 100% for osseous invasion.

For compartmental anatomy we refer to the article of Anderson MW [2] which will be discussed in more detail in Chap. 9.

The parameter "*growth rate*" is related to the aggressiveness of a soft tissue tumor and not to its malignancy grade.

Intratumoral hemorrhage is a rare finding, which can be observed in both benign and malignant lesions, and is difficult to differentiate from nontumoral soft tissue hematoma. In a study by Moulton et al., intratumoral hemorrhage was observed in 23 benign and in 5 malignant tumors among a total number of 225 masses. Hemorrhage was diagnosed on the basis of high signal on T1-weighted images, coupled with low or high signal on T2-weighted images, provided the tissue was not isointense to fat on all sequences. A low signal hemosiderin rim was interpreted as evidence of prior hemorrhage [36].

Although malignant tumors show increased vascularity and have large extracellular spaces, depending on tumoral activity or aggressiveness, we found no correlation between *degree and pattern of enhancement* and malignancy grade.

Erlemann et al. showed that dynamic contrast-enhanced studies are valuable in distinguishing benign from malignant lesions. On time-intensity plots, the increase in signal intensity was always lower than 100% for benign tumors and between 80% and 280% for malignant tumors.

Slopes with a greater than 30% increase in signal intensity per minute were seen in 84% of malignant tumors, and slopes with a lower than 30% increase in signal intensity per minute were seen in 72% of benign tumors. However, some overlap was observed. Largely necrotic malignant tumors showed slopes similar to those of benign tumors, while rapidly growing benign lesions such as myositis ossificans showed slopes similar to those of malignant ones [17, 18].

Although a statistically significant difference was found between the "first pass" slope values of benign and malignant lesions, pathological and angiographic findings indicated that first pass images reflect tissue vascularization and perfusion rather than benignity or malignancy. In 25% of the cases, the dynamic MR images provide new information for diagnosis, choice of biopsy site, and follow up during chemotherapy [50].

Ma et al. demonstrated that intratumoral enhancement patterns of malignant and benign masses differ because of differences in neovascularity and interstitial pressure. Malignant lesions showing increased neovascularity at their periphery and increased interstitial pressure at their center. Their results suggest that the rim-to-center differential enhancement ratio has potential as an additional parameter for the MRI differentiation of indeterminate musculoskeletal masses [31].

More recently Van der Woude et al. [46] prospectively analyzed the value of fast, dynamic, subtraction MRI in grading soft tissue tumors. They assessed the interval between arterial and early tumor enhancement (sensitivity of 91% and specificity of 72%), peripheral or diffuse enhancement (sensitivity of 73% and specificity of 97%) and the progression of enhancement (time-signal intensity curves) (sensitivity of 86% and specificity of 81%) in differentiation of benign from malignant soft tissue tumors. Most malignant soft tissue tumors exhibited an early and peripheral enhancement with a steep slope, an early maximum followed by a transition to a stable level or a slight decrease of signal intensity.

Tacikowska found that determination of the enhancement rate coefficient in percent per second (erc %/s) on dynamic MRI had a high sensitivity (93%) and high specificity (73%) in differentiating benign and malignant STT while the pattern of enhancement better correlated with vascularization and perfusion and the size of the interstitial space rather than with tumor's histology [41, 42]. In a second study the same author assessed the value of total tumor enhancement expressed as percent and found it less accurate than the erc %/s [41, 42].

The best results are obtained by Van Rijswijk et al. [47] using a multivariate logistic regression to identify the best combination of MR imaging parameters that might be predictive of malignancy. This multivariate analysis of 140 soft tissue tumors revealed that combined nonenhanced static and dynamic contrast-enhanced MR imaging parameters were significantly superior to nonenhanced MR imaging parameters alone and to nonenhanced MR imaging parameters combined with static contrast-enhanced MR imaging parameters in prediction of malignancy. The most discriminating parameters were presence of liquefaction, start of dynamic enhancement (time interval between start of arterial and tumor enhancement), and lesion size (diameter) (Fig. 11.6).

One of the reasons for the controversy about the value of dynamic contrast enhanced MRI refers to the small molecular weight of commonly used gadolinium chelates. In a recent study about dynamic contrast-enhanced MR imaging of mammary soft tissue tumors Daldrup et al. demonstrated that quantitative tumor microvascular permeability assays generated with macromolecular MRI contrast medium correlate closely with histologic tumor grade while no significant correlation was found using small-molecular gadopentetate. Gadopentetate-enhanced MRI is highly sensitive for tumor detection but has been shown to lack specificity for cancer grading [11].

The potential value of diffusion-weighted MRI in characterizing STT was studied by Van Rijswijk et al. They found that true diffusion coefficients of malignant STT were significantly lower than those of benign masses whereas ADC values between both groups were not significantly different [47].

11.2.2 Combined Parameters

Although most investigators failed to establish reliable criteria for distinguishing benign from malignant lesions, a combination of individual parameters (MR signal characteristics, morphology, internal architecture, growth pattern and other anatomic features) yields higher sensitivity and specificity [51]. Berquist et al. reported important criteria (size, margins, and homogeneity of signal intensity) predicting malignancy with a specificity of 82–96%, a negative predictive value of 92–96%, and a positive predictive value of 88–90% [5].

In a prospective analysis of 36 consecutive cases of soft tissue tumors by Ma et al., MRI was 100% sensitive but only 17% specific, with an accuracy of 58% in predicting malignancy. These authors found a wide variability in the appearance of benign and malignant lesions on MR images, with a poor correlation between "benign characteristics" and the benignity of the lesion [32].

Moulton et al. analyzed the imaging features of 225 soft tissue tumors (179 benign, 46 malignant) to evaluate the efficacy of MRI in distinguishing benign from malignant lesions. Univariate analysis of individual features and stepwise logistic regression analysis of combinations of imaging features were performed. Quantitative analysis showed that no single imaging feature or combination of features could reliably be used to distinguish benign from malignant lesions. With subjective analysis, a correct and specific diagnosis of benignity could be made in 44% of the 225 tumors. For the entire cohort the sensitivity for diagnosis of malignancy by subjective analysis was 78%, while the specificity was 89%. When benign tumors were excluded, the specificity decreased to 76%, whereas the sensitivity remained the same. The authors concluded that the accuracy of MRI declines when typically benign tumors are excluded from analysis. A significant percentage of malignant lesions may appear deceptively benign with the currently used criteria [36].

We performed multivariate statistical analysis to determine the accuracy of ten parameters, individually and in combination, for predicting malignancy. When the following signs were observed together, malignancy was forecast with a sensitivity of 81% and a specificity of 81%: absence of low signal intensity on T2-weighted images, signal inhomogeneity on T1-weighted images, and mean diameter of the lesion greater than 33 mm (Fig. 11.1). Malignancy was predicted with the highest sensitivity when a lesion had high signal intensity on T2-weighted images, was larger than 33 mm in diameter, and had an inhomogeneous signal intensity on T1-weighted images. Signs that had the greatest specificity for malignancy included the presence of tumor necrosis, bone or neurovascular involvement, and a mean di-

Table 11.2. Diagram of the "grading" results in absolute numbers with statistical workup (95% "confidence intervals" within brackets)

	Histology malignant	Histology benign		
MRI malignant	115 (0.1778–0.2460)	76 (0.1121–0.1703)	82% (0.7324–0.8839	Specificity
MRI benign	8 (0.0069–0.0291)	349 (0.5958–0.6761)	98% (0.9256–0.9989)	NPV
	93% (0.8602–0.9680)	60% (0.5019–0.6907)	548	Total
	Sensitivity	PPV		p<0.0001

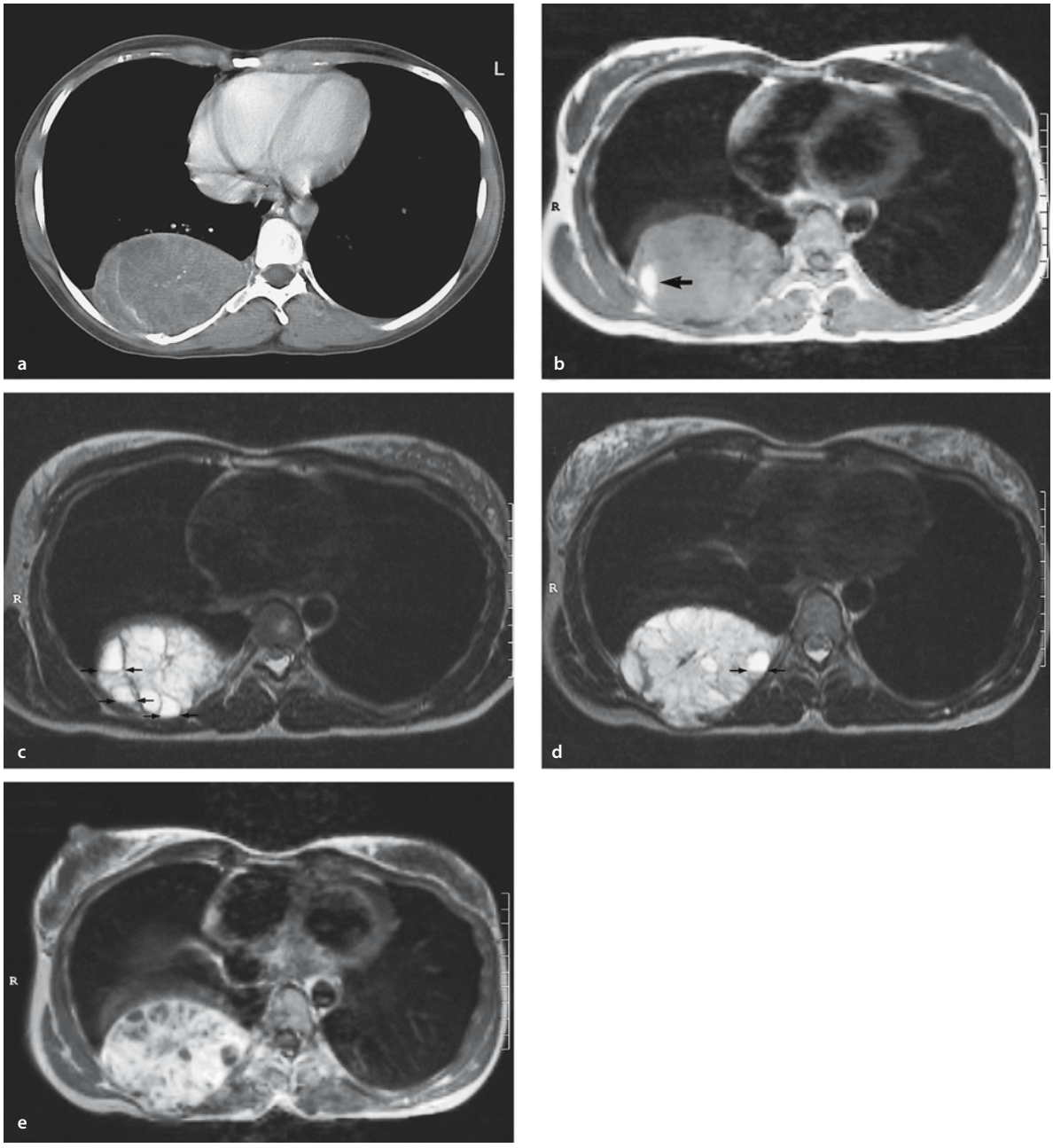

Fig. 11.1 a–e. Malignant peripheral nerve sheath tumor of the chest wall in a 29-year-old woman: **a** CT scan of the chest after I-contrast injection; **b** axial SE T1-weighted MR image; **c,d** axial SE T2-weighted MR image; **e** axial SE T2-weighted MR image after Gd-contrast injection. On CT scan of the chest there is a large, rounded and sharply demarcated mass located in the costovertebral gutter, with presence of intralesional calcifications and spoke-wheel-like enhancement after contrast injection (**a**). On T1-WI the lesion is inhomogeneous and of intermediate SI. There is a small area of high SI laterally within the mass (*arrow*) (**b**). On T2-WI there is again a spoke-wheel appearance of the lesion, there are multiple fluid-fluid levels, and rounded high SI areas (*small arrows*) on a background of intermediate to high SI (**c, d**). On T1-WI after contrast injection there is marked enhancement without enhancement of the rounded high SI areas on T2-WI (compare **d** with **e**). Large size (50×80×80 mm), extracompartmental extension and bone involvement, inhomogeneous distribution of SI and presence of amorphous calcifications within the lesion are parameters, predicting malignancy. Sharp margins and presence of intralesional hemorrhage are non-discriminatory parameters. Localization is in favor of a neurogenic tumor. Histologic diagnosis after resection confirmed the diagnosis of a malignant nerve sheath tumor (right 8th intercostal nerve)

ameter of more than 66 mm. Of the malignant lesions, 80% had irregular or partially irregular margins, while a similar percentage of benign masses had well-defined or partially irregular margins. The majority of both benign and malignant lesions showed moderate or strong enhancement, no predominant enhancement pattern emerged for either type of mass. In contrast to the study of Berquist et al., margin, signal homogeneity on T2-weighted images, signal intensity on T1-weighted images, shape, and enhancement pattern were statistically nondiscriminatory [14].

More recently we prospectively assessed the value of MRI in grading soft tissue tumors in a series of 548 untreated patients originating from a multi-institutional database, 123 with malignant and 425 with benign tumors. The thresholds to differentiate between malignant and benign STT are interpreted in a non quantitative way using grading parameters described in literature and mentioned before and, based on a fifteen year experience time of our research group. In this regard we obtained a sensitivity of 93%, a specificity of 82%, a negative predictive value of 98% and a positive predictive value of 60% in diagnosing malignancy (Table 11.2) [22].

11.3 Tissue Specific Diagnosis

Even though the primary concern of the referring physician is not histologic determination of tumor type but recognition of malignant features and distinction from benign counterparts, it was expected that MR imaging had great potential for the histological classification of soft tissue tumors because of its high intrinsic contrast resolution [8, 35, 36]. Unfortunately, the initial enthusiasm has not entirely been confirmed.

There are two reasons for this failure. First, MR images provide only indirect information about tumor histology by showing signal intensities related to some physicochemical properties of tumor components (e.g. fat, blood, water, collagen) and consequently reflect the gross morphology of the lesion rather than the underlying histology. Soft tissue tumors belonging to the same histological group may have a different composition or different proportions of tumor components resulting in different MR signals. This feature is well exemplified by the group of liposarcomas which can be well differentiated (lipomatous), myxoid, round cell or pleomorphic, or contain different proportions of these components. Only well differentiated liposarcomas are predominantly fatty, while the other histologic subtypes have less than 25% fat or no fat at all. As a consequence, there are no specific MRI characteristics for liposarcomas as a total group.

The second reason for the poor performance of MR in characterizing tumors histologically is the fact of time-dependent changes during natural evolution or as a consequence of therapy. Young desmoid tumors have a high water content and are highly vascularized, which results in high signal intensity on T2-weighted images. With aging they become more collagenous, which results in decreasing signal intensity. The same transformation is described for many tumors of fibrous tissue and also for the formerly named malignant fibrous histiocytomas. Furthermore, the signal intensity of large malignant tumors undergoes changes as a consequence of intratumoral necrosis and/or bleeding.

These limitations have prompted Kransdorf to state that "a correct histologic diagnosis reached on the basis of imaging studies is possible in only approximately one quarter of cases" [30].

In an early retrospective study on characterization Balzarini [3] reported that most lesions have a non-specific MRI appearance, except for lipomatous and fibrous lesions. On the other hand, in a retrospective study of 134 masses and pseudo-masses of the hand and wrist Capelastegui et al. reported an accurate diagnosis with differentiation of tumor-like lesions from genuine tumor [8].

In their prospective study on grading and characterization of 95 lesions (50 benign and 45 malignant) Berquist et al. predicted the exact histology of the lesion in 22% and in 58% of the benign group. Predicting histology of malignant lesions was not successful at all [5].

In the largest, partially prospective study Moulton et al. were able to predict the diagnosis confidently and correctly in 44% of 225 cases of soft tissue tumors. The majority of these cases were benign lesions such as lipomas, hemangiomas and arteriovenous malformations, benign neural tumors, periarticular cysts, hematomas, pigmented villonodular synovitis (PVNS), giant cell tumors of tendon sheath, and abscesses [36].

More recently Gielen et al. [22] reported on a series of 548 histologically proven soft tissue tumors in which a correct tissue specific diagnosis on MRI was made in 294 out of 425 benign tumors and in 47 out of 123 malignant tumors.

Table 11.3. Statistical work-up of tissue specific diagnosis [22]

	Sensitivity	Specificity	PPV	NPV
Benign+malignant	67%	98%	70%	98%
Benign	75%	98%	76%	98%
Malignant	37%	96%	40%	96%

Statistical workup for the whole cohort of benign and malignant tumors are summarized in Table 11.3. A correct tissue specific diagnosis was included in the differential diagnosis made on MRI (maximum of three possibilities) in 367 (67%) of the cases.

To determine whether potential MR imaging features suggest a specific diagnosis, we reviewed the current literature and found a large number of specific features, most of which were unfortunately of poor sensitivity. As for grading, the evaluation of a combination of different parameters seems more useful than the evaluation of individual parameters.

The usefulness of the relative prevalence, age at presentation, sex distribution and zonal distribution of 18,677 benign and 12,370 malignant soft tissue tumors was studied by Kransdorf in a large referral population [27, 28]. Approximately 70% of benign lesions were classified into eight diagnostic categories : lipoma and lipoma variants (16%), fibrous histiocytoma (13%), nodular fasciitis (11%), hemangioma (8%), fibromatosis (7%), neurofibroma (5%), schwannoma (5%), and giant cell tumor of tendon sheath (4%). In total, 52 diagnostic categories were used for analysis. It was possible to group approximately 80% of all benign tumors in the seven most common diagnostic categories for each age and location.

More than 80% of the malignant lesions were classified into eight diagnostic categories: malignant fibrous histiocytoma (24%), liposarcoma (14%), leiomyosarcoma (8%), malignant schwannoma (6%), dermatofibrosarcoma protuberans (6%), synovial sarcoma (5%), fibrosarcoma (5%) and sarcoma, not classified further (12%). In total, 31 malignant diagnostic categories were used for analysis. It was possible to group approximately 79% of all malignant tumors under the five most common diagnoses for each age and location (Tables 11.4 and 11.5) [27, 28].

In this study there were inherent biases, which the author himself recognized. To begin with, there is a relatively high percentage of malignant tumors in this series. The consultative nature of the cases probably introduced a preference for difficult case material. Second, the reported data reflect lesions found at biopsy. Many small superficial lesions are excised or sampled without imaging. Lesions in this group include dermatofibrosarcoma protuberans, giant cell fibroblastoma and atypical fibroxanthoma. In our own series of more than 2500 soft tissue tumors, these lesions were indeed rarely seen. Nevertheless, the tables from Kransdorf's paper are highly useful and should be accessible to all radiologists interested in soft tissue tumor pathology.

Signal intensity on different pulse sequences may be helpful in making a more specific diagnosis. And although most tumors display intermediate signal, similar to that of muscle on T1-weighted images, intermediate to high with respect to fat on T2-weighted images [24], we found that a large number of soft tissue tumors can be classified into five diagnostic categories, according to their signal intensity on T1- and T2-weighted images [Table 11.9]. Combination of signal intensities have been described in neurofibromas where a central low signal on T2-weighted images is combined with a high signal of the surrounding periphery. This so called "target" pattern is characteristic for neurofibromas, rarely seen in schwannomas and almost never described in malignant nerve sheath tumors [9, 51].

We observed an inverted target sign (high signal intensity center combined with a low signal periphery) in nodular fasciitis and metastasis.

The use of intravenously injected paramagnetic contrast agents is valuable in the detection and staging of soft tissue tumors, but neither the intensity nor the pattern of enhancement contributes to further tissue specific diagnosis of these lesions [25]. Dynamic contrast studies are useful in assessing the response of soft tissue tumors to chemotherapy and in differentiating postoperative edema from recurrent tumor. First pass imaging introduced by Verstraete may aid in differentiating hemangioma from arteriovenous malformation [50].

Multi-institutional approach allows to gain the best experience of a rare pathology such as soft tissue tumors. In this regard Marti-Bonmati and coworkers introduced a STT decision support system based on web services architecture. The system uses a pattern recognition technology (artificial neural networks, support vector machine, k-nearest neighbor) and epidemiological information to discriminate between benign and malignant tumors. After the systems had learned by using training samples (with 302 cases), the clinical decision support system was tested in the diagnosis of 128 new STT cases with a 88–92% efficacy [33].

A comparable system was introduced by A. De Schepper and coworkers by organizing the "Belgian Soft Tissue Neoplasm Registry" (BSTNR), a multi-institutional database of soft tissue tumors with the cooperation of most MR centers in Belgium.

As a guideline for the reader we have summarized the value of different parameters such as preferential location (Table 11.6), shape (Table 11.7), presence of signal voids (Table 11.8), signal intensities on different pulse sequences (Table 11.9), concomitant diseases (Table 11.11), fluid-fluid levels (Table 11.12), and multiplicity (Table 11.10) in concise tables.

The above-mentioned and other morphological features characteristic for some specific tumors are highlighted and illustrated in Fig. 11.1 until 11.14 and described in the respective chapters.

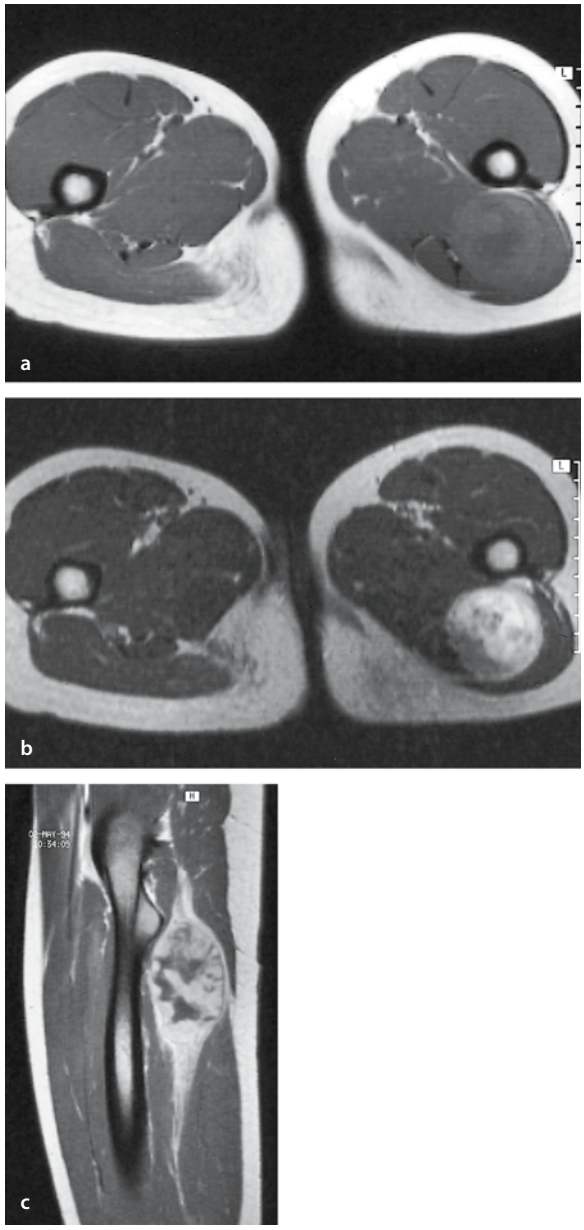

Fig. 11.2 a–c. Malignant peripheral nerve sheath tumor (MPNST) of the thigh in a 22-year-old woman: **a** axial SE T1-weighted MR image; **b** axial SE T2-weighted MR image; **c** sagittal SE T1-weighted MR image after Gd-contrast injection. There is a mass lesion in between the left adductor and gluteal muscles. The lesion is slightly inhomogeneous on T1-WI and definitely inhomogeneous on T2-WI. Sagittal image after contrast injection shows the fusiform shape of the lesion, the location on the course of the sciatic nerve and the presence of intratumoral necrosis. Imaging features are suggestive for a malignant (diameter of more than 80 mm, inhomogeneity, changing homogeneity, intratumoral necrosis) neurogenic (fusiform, along the course of a major nerve) tumor. Histologic examination after resection confirmed the diagnosis of MPNST

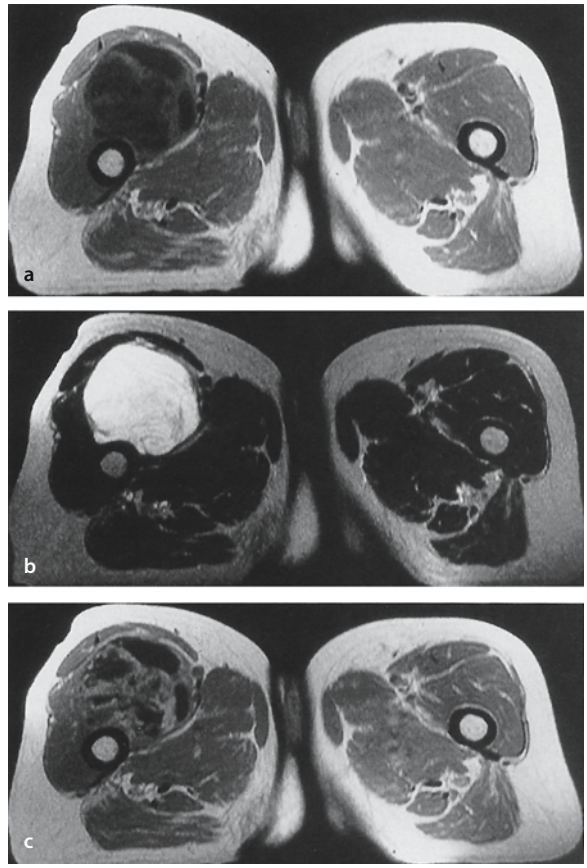

Fig. 11.3 a–c. Fibromyxoid sarcoma of the right quadriceps muscle in a 64-year-old woman: **a** axial SE T1-weighted MR image; **b** axial SE T2-weighted MR image; **c** axial SE T1-weighted MR image after gadolinium contrast injection. The huge mass is inhomogeneous on SE- T1-WI (**a**), has a high signal intensity on SE-T2-WI (**b**) and shows a peripheral enhancement on SE- T1-WI after Gd contrast (**c**). Localization, size of the lesion, signal intensities on different pulse sequences and behavior after Gd contrast injection with peripheral and septal enhancement, are highly suggestive of a malignant tumor

Table 11.4 Distribution of common benign soft tissue tumors by anatomic location and age

Age (years)	Hand and wrist	%	Upper extremity	%	Axilla and shoulder	%	Foot and ankle	%	Lower extremity	%
0–5	Hemangioma	15	Fibrous hamartoma of infancy	16	Fibrous hamartoma of infancy	29	Granuloma annulare	30	Granuloma annulare	23
6–15	Fibrous histiocytoma	14	Fibrous histiocytoma	23	Fibrous histiocytoma	34	Fibromatosis	23	Hemangioma	22
16–25	GCTTS	20	Nodular fasciitis	35	Fibrous histiocytoma	36	Fibromatosis	22	Fibrous histiocytoma	24
26–45	Fibrous histiocytoma	18	Nodular fasciitis	38	Lipoma	28	Fibromatosis	21	Fibrous histiocytoma	25
46–65	GCTTS	23	Nodular fasciitis	20	Lipoma	58	Fibromatosis	25	Lipoma	23
66 and over	GCTTS	21	Lipoma	22	Lipoma	58	Fibromatosis	14	Lipoma	26

Age (years)	Hip, groin & buttocks	%	Head and neck	%	Trunk	%	Retroperitoneum	%
0–5	Fibrous hamartoma of infancy	20	Nodular fasciitis	20	Hemangioma	18	Lipoblastoma	37
6–15	Nodular fasciitis	27	Nodular fasciitis	33	Nodular fasciitis	28	Lymphangioma	37
16–25	Neurofibroma	16	Nodular fasciitis	21	Nodular fasciitis	24	Fibromatosis	20
26–45	Lipoma	17	Lipoma	29	Lipoma	19	Schwannoma	23
46–65	Lipoma	35	Lipoma	46	Lipoma	44	Schwannoma	19
66 and over	Lipoma	21	Lipoma	50	Lipoma	42	Schwannoma	26

GCTTS, giant cell tumor of tendon sheath.
From Kransdorf [28].

Table 11.5 Distribution of common malignant soft tissue tumors by anatomic location and age

Age (years)	Hand and wrist	%	Upper extremity	%	Axilla and shoulder	%	Foot and ankle	%	Lower extremity	%
0–5	Fibrosarcoma	45	Fibrosarcoma	29	Fibrosarcoma	56	Fibrosarcoma	45	Fibrosarcoma	45
6–15	Epithelioid sarcoma	21	Angiomatoid MFH	33	Angiomatoid MFH	21	Synovial sarcoma	21	Synovial sarcoma	22
16–25	Epithelioid sarcoma	29	Synovial sarcoma	23	Synovial sarcoma	18	Synovial sarcoma	30	Synovial sarcoma	22
26–45	MFH	18	MFH	28	DFSP	33	Synovial sarcoma	26	Liposarcoma	28
46–65	MFH	19	MFH	46	MFH	35	MFH	25	MFH	43
66 and over	MFH	35	MFH	60	MFH	50	Kaposi's sarcoma	37	MFH	55

Age (years)	Hip, groin & buttocks	%	Head and neck	%	Trunk	%	Retroperitoneum	%
0–5	Fibrosarcoma	32	Fibrosarcoma	37	Fibrosarcoma	26	Fibrosarcoma	20
6–15	Angiomatoid MFH	21	Rhabdomyosarcoma	26	Angiomatoid MFH	15	Rhabdomyosarcoma	31
16–25	Synovial sarcoma	18	MFH	19	DFSP	23	Malignant schwannoma	20
26–45	Liposarcoma	18	DFSP	30	DFSP	30	Leiomyosarcoma	32
46–65	Liposarcoma	24	MFH	28	MFH	31	Liposarcoma	33
66 and over	MFH	46	MFH	34	MFH	44	Liposarcoma	39

DFSP, dermatofibrosarcoma protuberans; MFH, malignant fibrous histiocytoma (myxofibrosarcoma).
From Kransdorf [27].

Table 11.6. Preferential location of soft tissue tumors

Location		Tumor
Neck		Cystic hygroma – lymphangioma (infants)
		Capillary hemangioma (infants)
		Myofibroma (children)
		Infantile desmoid fibromatosis (children)
	Dorsal neck	Nuchal fibroma
	Sternocleidomastoid muscle	Fibromatosis colli (children)
	Carotid bifurcation	Glomus tumor
Trunk	Axilla	Cystic hygroma – lymphangioma
	Subscapular	Elastofibroma
	Spinoglenoid notch	Ganglion cyst
	Paraspinal gutter	Neurogenic tumor
Abdomen	Rectus abdominis muscle	Abdominal desmoid
	Costal gutter – paraspinal gutter	Neurogenic tumor
	Psoas muscle, parapsoatic	Plexiform neurofibroma
Pelvis	Presacral	Plexiform neurofibroma
	Buttock, lateral aspect	Desmoid
		Injection granuloma
	Coccyx	Extraspinal ependymoma
Upper limb	Deltoid, subcutaneous	Desmoid
		Injection granuloma
	Forearm, volar aspect	Nodular fasciitis
	Medial epitrochlear lymph node	Cat scratch disease
	Wrist	Ganglion cyst
	Wrist, volar aspect	Fibrolipohamartoma of median nerve
	Hand	Gouty tophi
	Hand, volar aspect	Palmar fibromatosis
		Fibrolipohamartoma of median nerve
	Hypothenar	Hypothenar hammer syndrome
	Finger	Macrodystrophia lipomatosa
	Finger, volar aspect	Giant cell tumor of tendon sheath
	Finger, dorsal aspect	Digital fibroma (children)
	Finger, tip	Epidermoid cyst
		Glomus tumor
Lower limb	Flexor aspect, along major nerves	Schwannoma
	Thigh	Fibrohamartoma of infancy (infants)
		Alveolar soft part sarcoma (adults)
		Sarcoma (liposarcoma) (older men)
	Knee	Synovial hemangioma
		Pigmented villonodular synovitis (young, middle aged men)
		Lipoma arborescens (older men)
	Knee, popliteal fossa	Pigmented villonodular synovitis
		Baker's cyst
		Synovial cyst
		Ganglion cyst
		Meniscal cyst
		Nerve sheath tumor
		Aneurysm of popliteal artery
	Knee, tibio-fibular joint	Ganglion cyst
	Ankle	Ganglion cyst
	Foot, extensor aspect	Ganglion cyst
	Sole	Synoviosarcoma (young adults)
		Plantar fibromatosis
	Heel	Clear cell sarcoma
	Metatarsals	Morton's neuroma (women)
	Toes	Giant cell tumor of tendon sheath
Upper and lower limb		Fibrous histiocytoma
		Myxofibrosarcoma
		Myositis ossificans
	Extensor aspect	Leiomyoma (young adults)
Joints, periarticular		Synovial hemangioma
		Amyloidosis
		Lipoma arborescens
		Pigmented villonodular synovitis
		Synoviosarcoma
Tendons	(Achilles tendon, bilateral)	Xanthoma
		Giant cell tumor of tendon sheath
Course of major nerves		Nerve sheath tumors
Cutis, subcutis		Desmoid
		Neurofibroma
		Nodular fasciitis
		Dermatofibrosarcoma protuberans
		Granular cell tumor

Table 11.7. Shape

Fusiform (ovoid)	Neurofibroma Lipoma
Dumbbell	Neurofibroma Desmoid
Moniliform	Neurofibroma Synovial – ganglion cyst
Round	Cyst Schwannoma
Serpiginous	Hemangioma
Soap bubbles – cauliflower	Lipoma arborescens
Nodular	Fibromatosis (plantaris, palmaris)
Branching (bilateral) Finger-like	Plexiform neurofibroma

Table 11.8. Intratumoral signal void

Flow	Hemangioma (capillary) Arteriovenous malformation
Calcification	Hemangioma (phlebolith) Lipoma (well-differentiated and dedifferentiated) Desmoid Cartilaginous tumors Osteosarcoma of soft tissue Synoviosarcoma (poorly defined, amorphous) Chordoma Alveolar soft part sarcoma Myositis ossificans (marginal-zonal)
High content of collagen	Desmoid

Table 11.9. Groups of STT according to their signal intensities on T1- and T2-weighted images

Group I High signal intensity on T1-weighted images, intermediate signal intensity on T2-weighted images	Lipoma Liposarcoma Lipoblastoma Hibernoma Elastofibroma Fibrolipohamartoma Metastasis of melanoma (melanin) Clear cell sarcoma (melanin)
Group II High signal intensity on T1-weighted images, high signal intensity on T2-weighted images	Hemangioma Lymphangioma Subacute hematoma Small arteriovenous malformation
Group III Low signal intensity on T1-weighted images, high signal intensity on T2-weighted images	Cyst Myxoma Myxoid liposarcoma Sarcoma
Group IV Intermediate signal intensity on T1-weighted images, high signal intensity on T2-weighted images	Neurogenic tumor Desmoid Tumors of muscular origin
Group V Low to intermediate signal intensity on T1-weighted images, low to intermediate signal intensity on T2-weighted images	Desmoid and other fibromatoses Pigmented villonodular synovitis Morton's neuroma Fibrolipohamartoma Giant cell tumor of tendon sheath Acute hematoma (few days) Old hematoma Xanthoma High flow arteriovenous malformation Mineralized mass Scar tissue Amyloidosis Granuloma annulare Lymphoma High grade malignancies

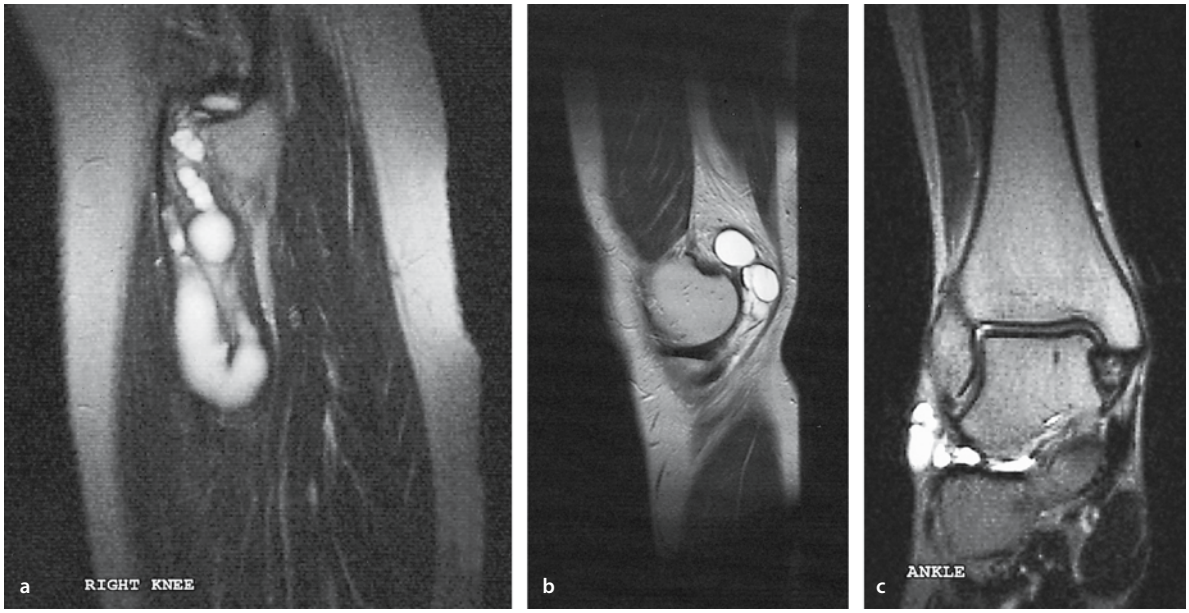

Fig. 11.4 a–c. Synovial cysts in three different patients: **a** sagittal SE T2-weighted MR image of the lower leg (34-year-old woman); **b** sagittal SE T2-weighted MR image of the knee (31-year-old woman); **c** coronal SE T2-weighted MR image of the ankle (46-year-old woman). All three lesions have a beaded appearance, very high SI on T2-WI and show connection with the neighboring joint. These imaging features make the diagnosis of a synovial cyst almost certain

Fig. 11.5 a–d. Four examples of soft tissue tumors having a characteristic localization and signal intensities on MRI: **a** giant cell tumor of the tendon sheath at the volar aspect of a finger with low signal intensity on SE- T1 and SE- T2-WI (not shown); **b** synovial hemangioma of the knee with intra-articular localization, characteristic serpiginous morphology and high signal intensity on fat suppressed T2-WI; **c** elastofibroma dorsi of the subscapular region with a characteristic lenticular shape, and mixed signal intensities (fat and fibrous tissue) on SE-T1-WI; **d** malignant nerve sheath tumor of the sciatic nerve with fusiform shape, "fat split" sign, localization on the course of a major nerve (neurogenic tumor) and peripheral enhancement and/or central necrosis (malignant lesion)

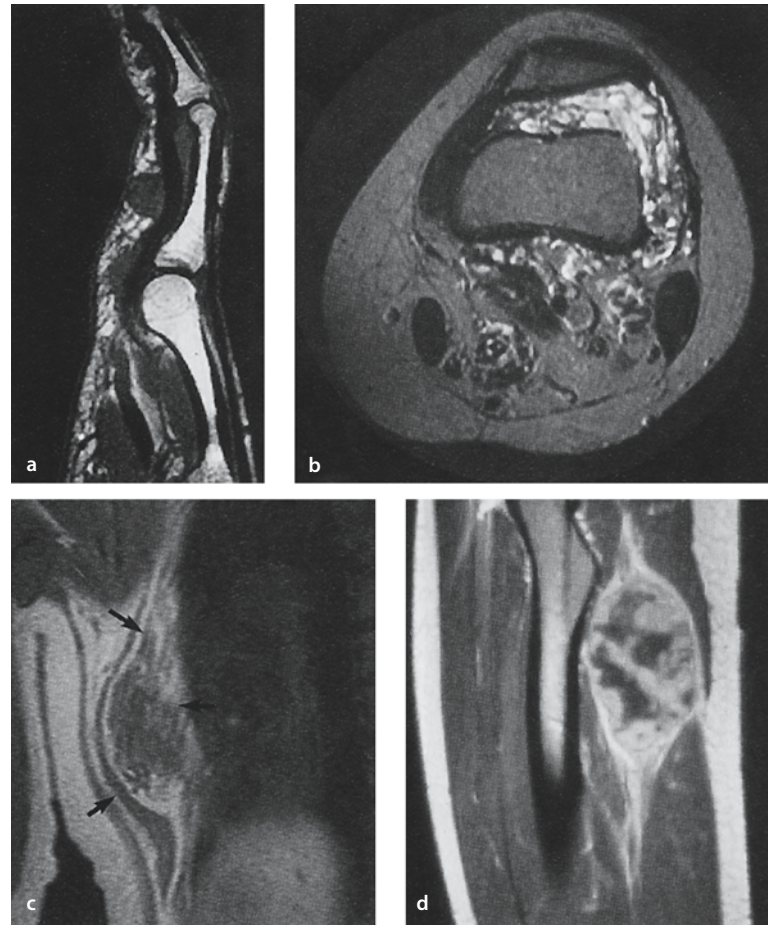

Table 11.10. Multiplicity

Venous malformation
Lipoma 5–8 %
Lipoma of tendon sheath (50 %)
Desmoid
Neurofibroma
Myxoma
Metastasis
Dermatofibrosarcoma protuberans
Kaposi's sarcoma

Table 11.12. Fluid-fluid levels

Hemangioma
Cystic lymphangioma
Synoviosarcoma
Myxoma
Hematoma
Myositis
Metastasis

Table 11.11. Concomitant diseases

Concomitant osseous involvement	Pigmented villonodular synovitis Lymphoma Desmoid Angiomatosis Parosteal lipoma Myofibromatosis (children) Juvenile hyalin fibromatosis (children)
Maffucci's disease	Cavernous hemangioma(s)
Fibrous dysplasia (Mazabraud)	Myxoma(s)
Neurofibromatosis	Schwannoma(s) Neurofibroma(s)
Gardner's syndrome	Fibromatosis
Dupuytren's disease (flexion contractures)	Palmar fibromatosis
Macrodystrophia lipomatosa of the digits	Fibrolipohamartoma of the median nerve
Familial hypercholesterolemia	Xanthoma
Normolipidemia+lymphoma or granuloma	Cutaneous xanthoma
Multiple myeloma	Amyloidosis
Turner's syndrome	Lymphangioma
Diabetes+degenerative joint disease+trauma	Lipoma arborescens

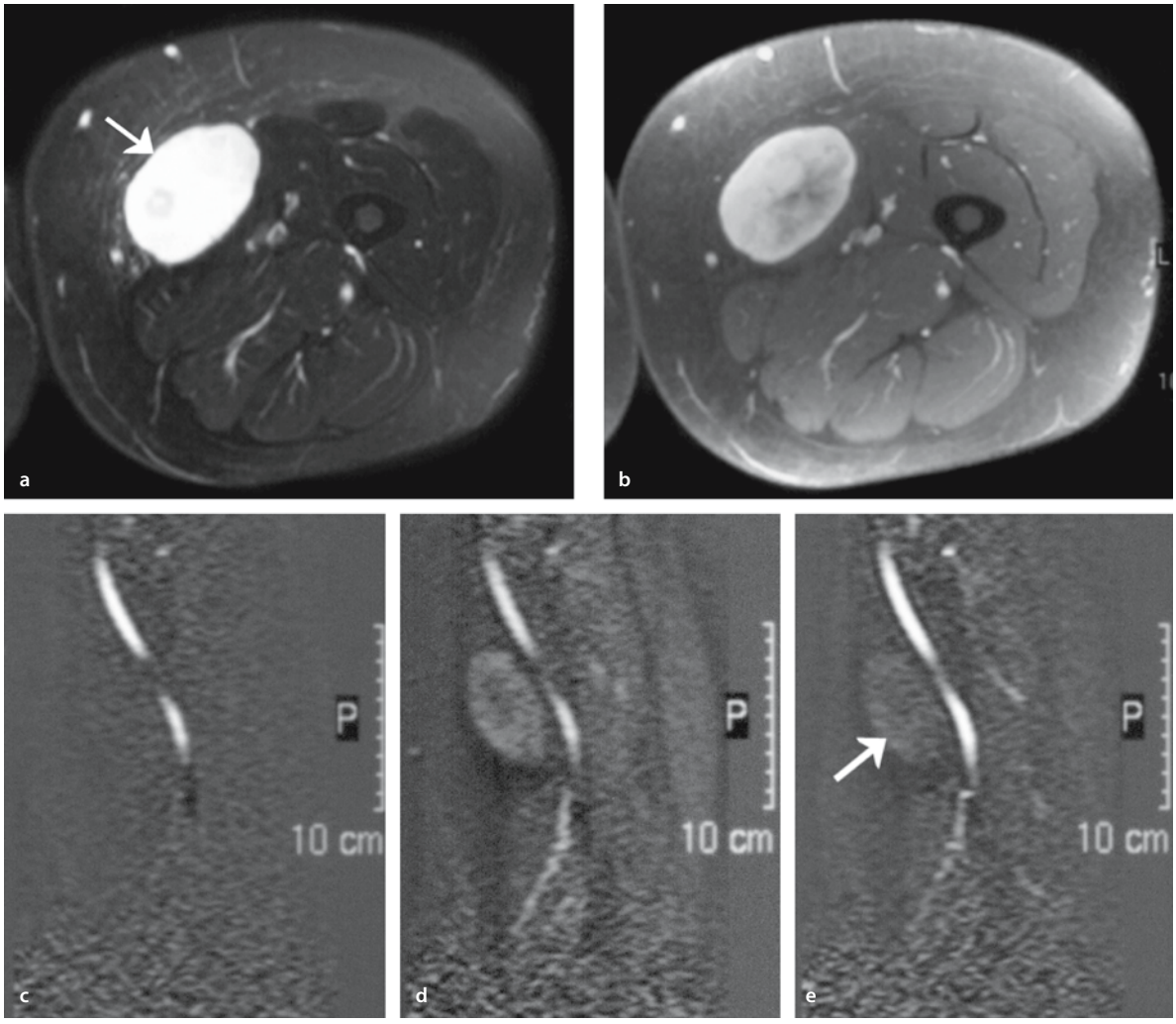

Fig. 11.6 a–e. Myxoid round cell liposarcoma: **a** axial SE T2-weighted MR image with fat suppression; **b** axial SE- T1-weighted MR image after Gd contrast administration with fat suppression; **c–e** dynamic MR sequence, subtraction images at the same level. **c.** Arrival of the bolus in the femoral artery. **d.** Image obtained 6 s later than **c. e.** Image obtained 30 s later than **d**. Early and intense enhancement in favor of a malignant soft tissue tumor [Courtesy of C.S.P van Rijswijk et al. Radiology (2004) 233:493–502]

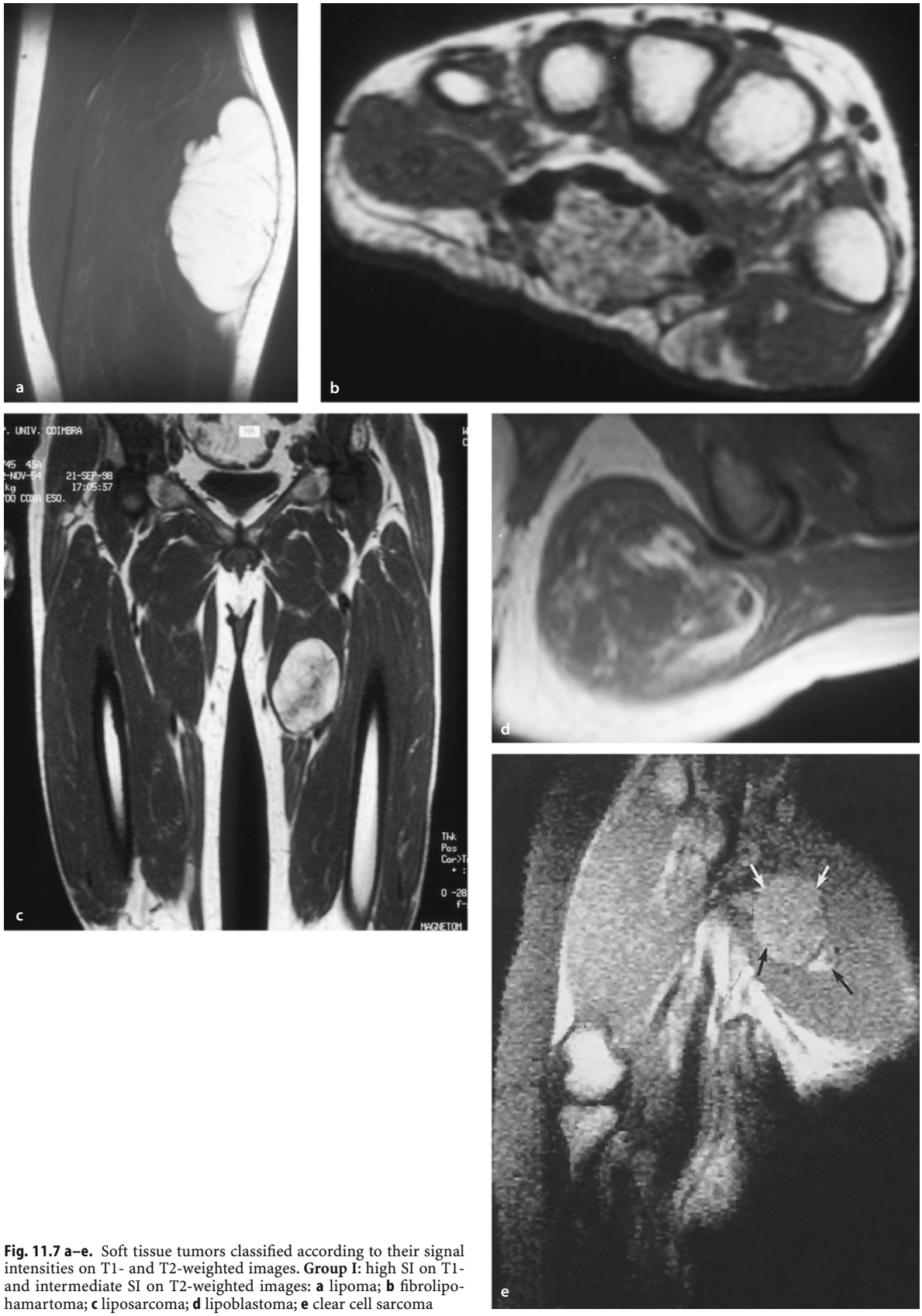

Fig. 11.7 a–e. Soft tissue tumors classified according to their signal intensities on T1- and T2-weighted images. **Group I**: high SI on T1- and intermediate SI on T2-weighted images: **a** lipoma; **b** fibrolipohamartoma; **c** liposarcoma; **d** lipoblastoma; **e** clear cell sarcoma

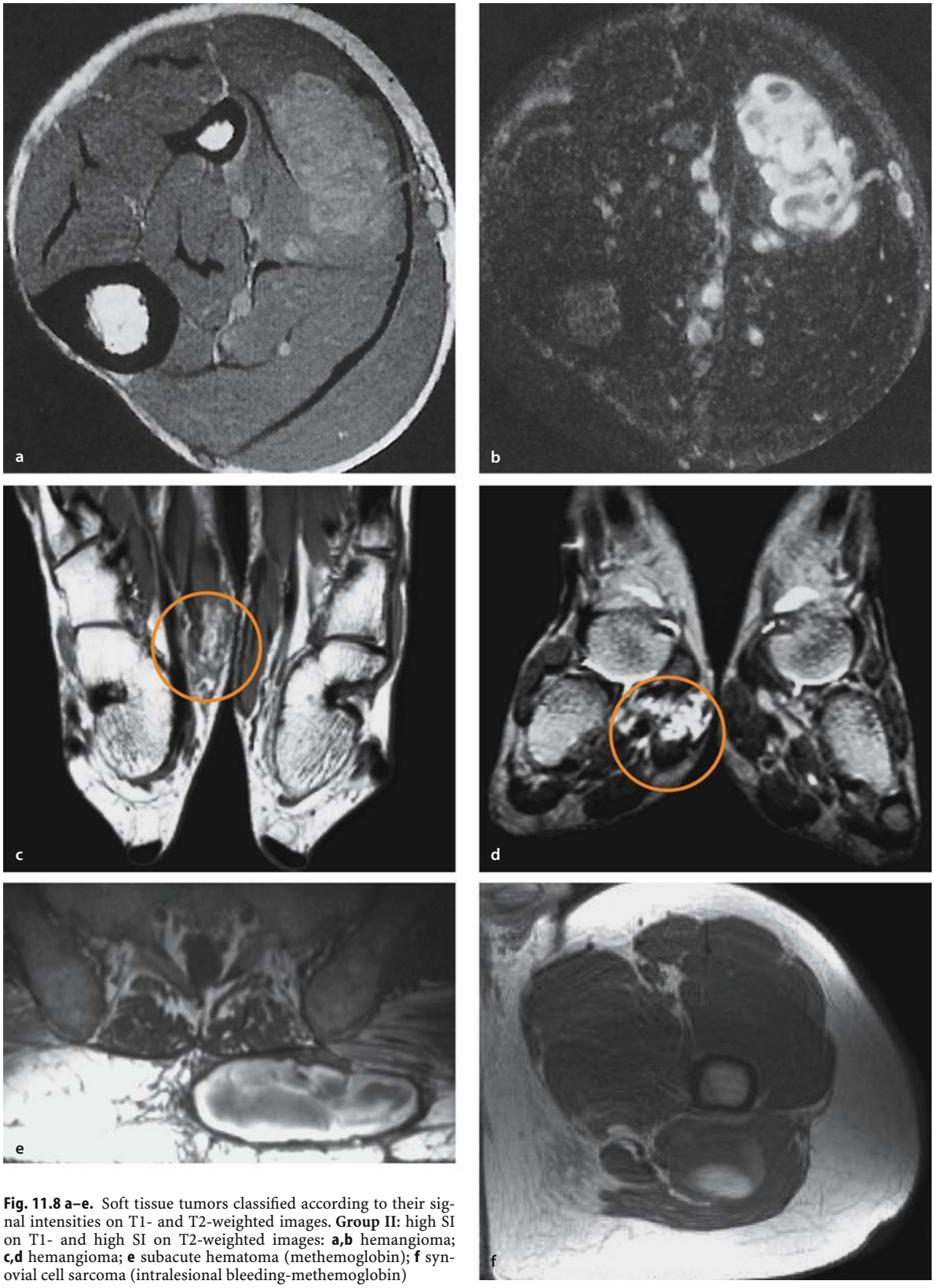

Fig. 11.8 a–e. Soft tissue tumors classified according to their signal intensities on T1- and T2-weighted images. **Group II**: high SI on T1- and high SI on T2-weighted images: **a,b** hemangioma; **c,d** hemangioma; **e** subacute hematoma (methemoglobin); **f** synovial cell sarcoma (intralesional bleeding-methemoglobin)

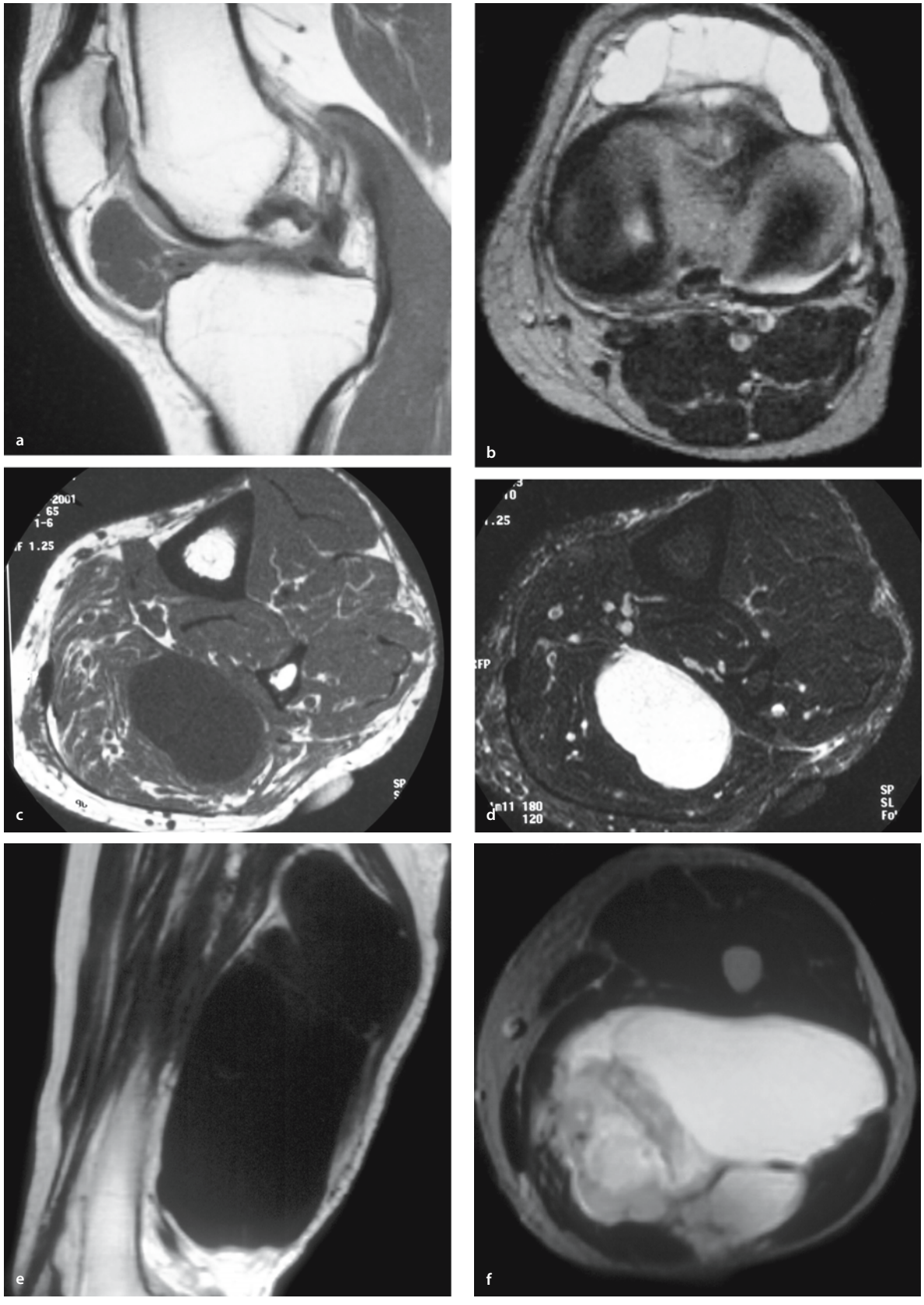

Fig. 11.9 e,f. Soft tissue tumors classified according to their signal intensities on T1- and T2-weighted images. **Group III:** low SI on T1- and high SI on T2-weighted images: **a,b** meniscal cyst; **c,d** myxoma; **e,f** myxoid liposarcoma

Fig. 11.10 a–d. Soft tissue tumors classified according to their signal intensities on T1- and T2-weighted images. **Group IV:** intermediate SI on T1- and high SI on T2-weighted images: **a,b** schwannoma (T1-WI / T2-WI); **c,d** nodular fasciitis (T1-WI/T2 WI)

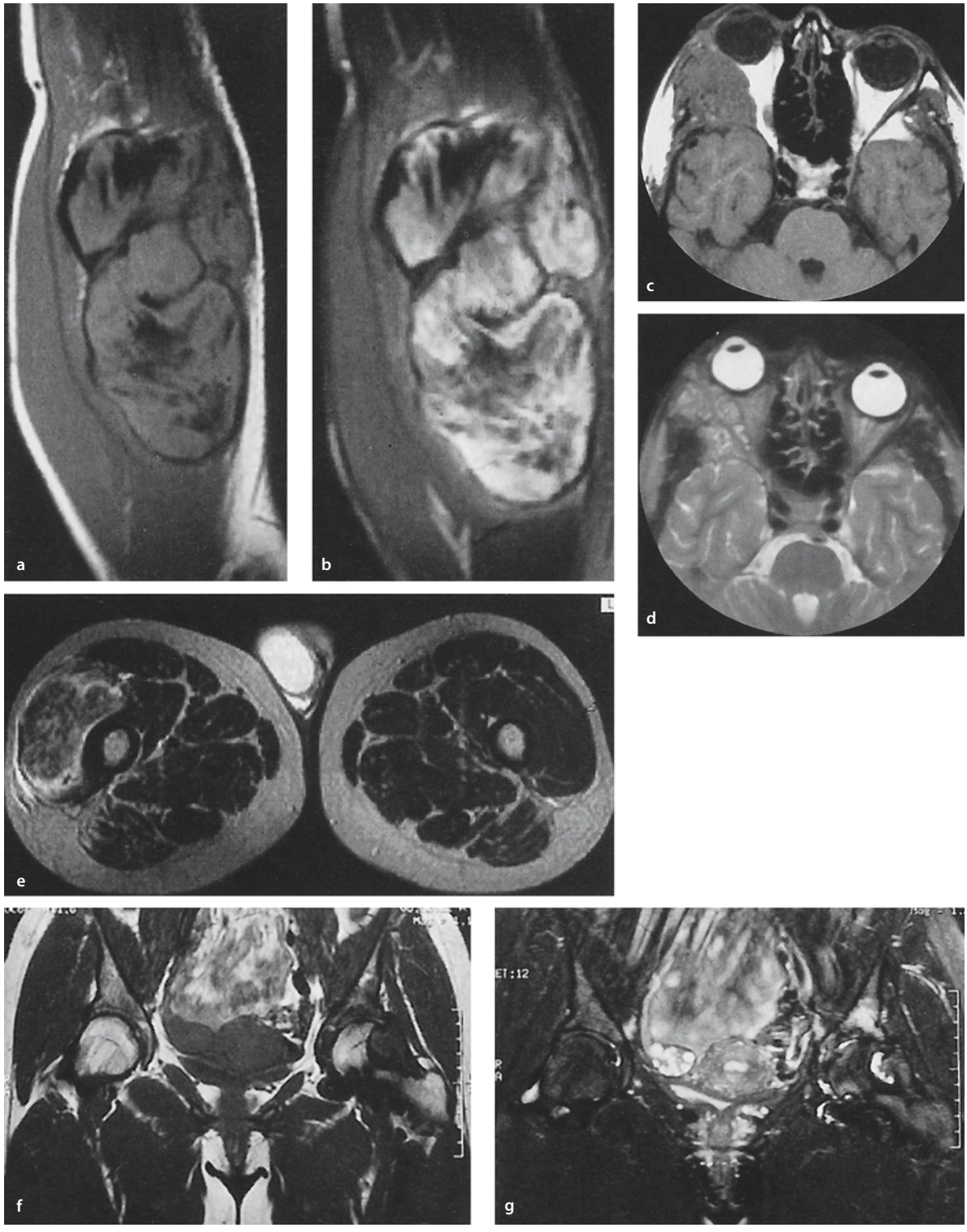

Fig. 11.11 a–i.

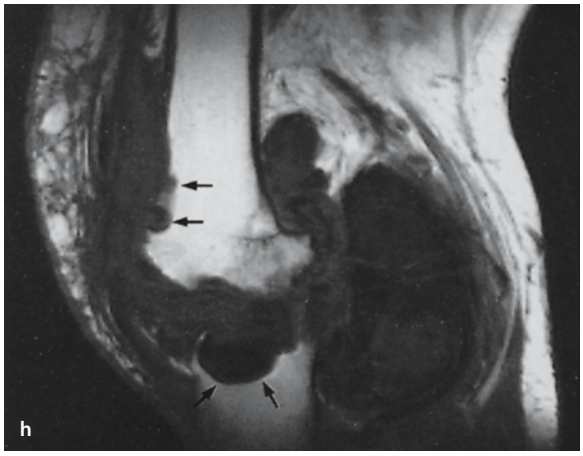

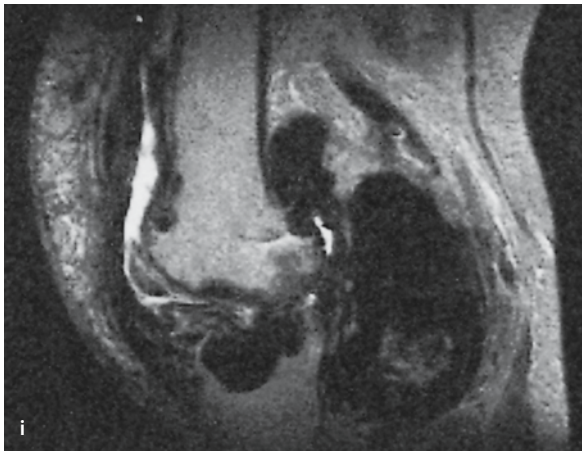

Fig. 11.11 h,i. Soft tissue tumors classified according to their signal intensities on T1- and T2-weighted images. **Group V**: low SI on T1- and low SI on T2-weighted images: **a,b** desmoid tumor (collagen); **c,d** rhabdomyosarcoma (high cellularity, decreased amount of intra- and extracellular water); **e** old hematoma (hemosiderin); **f,g** pigmented villonodular synovitis (hemosiderin); **h,i** pigmented villonodular synovitis (hemosiderin)

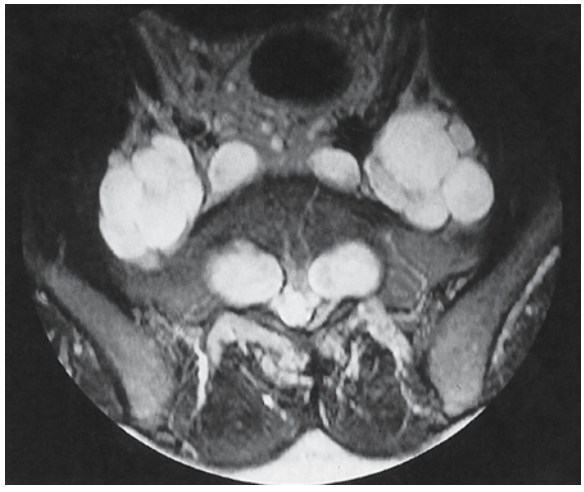

Fig. 11.12. Multiple neurofibromata of the presacral region and sacral spinal canal in a case of neurofibromatosis I presenting with a moniliform masses of high signal intensity on T2-WI.

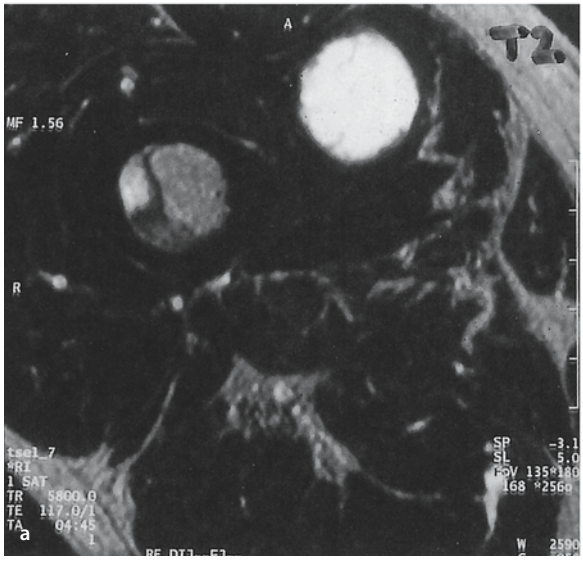

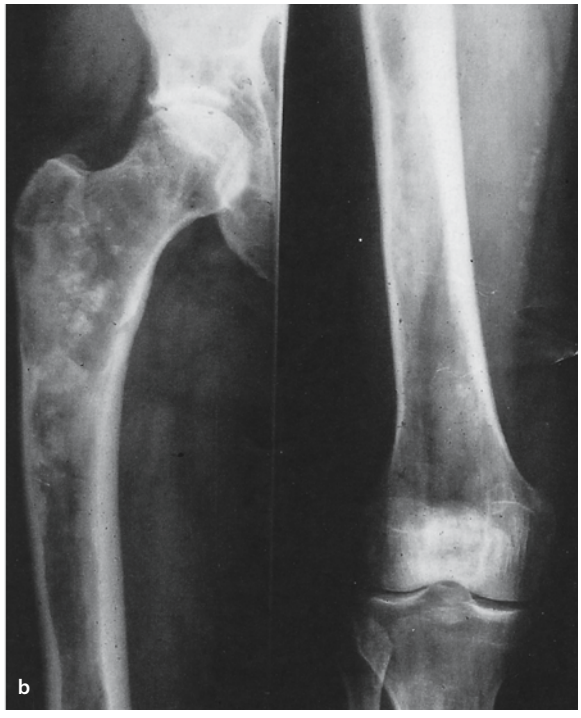

Fig. 11.13 a,b. Myxoma of the thigh (**a**) in a patient with fibrous dysplasia of the right femur (**b**) (Mazabraud's syndrome). Adjacent to the pathological right femur there is a rounded soft tissue mass with high signal intensity on SE-T2-WI

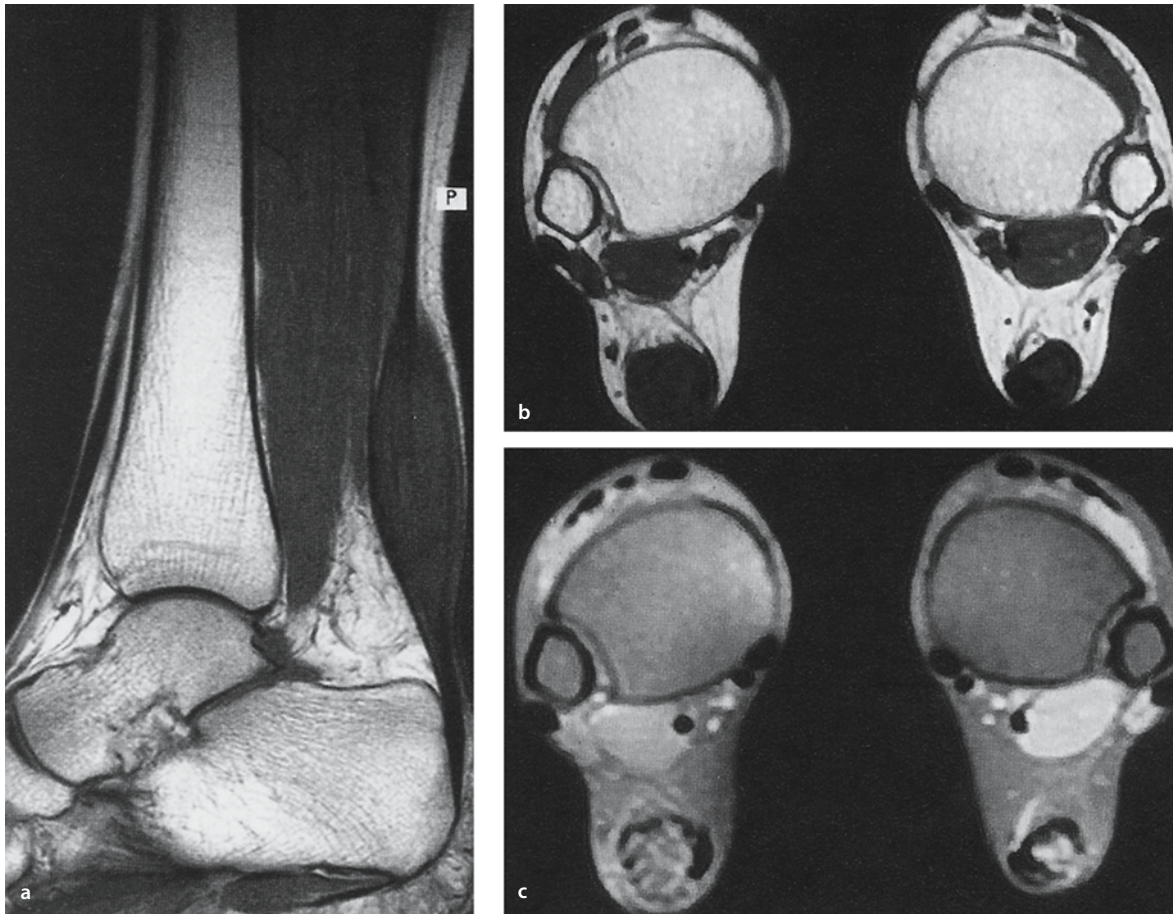

Fig. 11.14 a–c. Xanthoma of both Achilles tendons in a patient with familial hypercholesterolemia. Both lesions are fusiform on sagittal images (**a**), have a speckled appearance on axial SE- T1-WI (**b**) and the signal of intratendinous xanthomatous areas is not reduced on fat suppressed T1- WI (**c**)

Things to remember

1. Most soft tissue tumors are benign (60-75%). The major role of grading consists in recognizing benign soft tissue tumors, which will be excluded from further invasive diagnostic and therapeutic procedures.
2. Accuracy of individual (MR imaging-) parameters is low except for dynamic contrast-enhanced MR parameters which allow the best differentiation between benign and malignant soft tissue tumors.
3. Best results are obtained by combining individual grading parameters (sensitivity 93%/specificity 82%).
4. Besides age and location, shape, signal intensities on different pulse sequences, presence of signal voids, presence of fluid-fluid levels, multiplicity and knowledge of associated diseases, are major tissue specific parameters. Here also, combination of different parameters increases imaging performance.
5. Five groups of soft tissue tumors are defined, according to their signal intensities on T1- and T2-weighted MR images. High SI on T1- and low SI on T2-weighted images have the best predictive value concerning tissue specific diagnosis.
6. Multi-institutional approach of soft tissue tumors guarantees best diagnostic and therapeutic results.

References

1. Alexander A, Nazarian L, Feld R (1997) Superficial soft tissue masses suggestive of recurrent malignancy: sonographic localization and biopsy. AJR Am J Roentgenol 169:1449–1451
2. Anderson MW, Temple HT, Dussault RG, Kaplan PA (1999) Compartmental anatomy: relevance to staging and biopsy of musculoskeletal tumors. Am J Roentgenol 173:1663–1671
3. Balzarini L, Ceglia E, Petrillo R, Tesoro Tess JD, Reitano A, Musumeci R (1989) Magnetic resonance in neoplasms of the adipose, fibrous and muscular tissues. Radiol Med 77:87–93
4. Bass J, Korobkin M, Francis I, Ellis J, Cohan R (1994) Retroperitoneal plexiform neurofibromatosis: CT findings. AJR Am J Roentgenol 163:617–620

5. Berquist T, Ehman R, King B, Hodgman C, Ilstrup D (1990) Value of MR imaging in differentiating benign from malignant soft-tissue masses: study of 95 lesions. AJR Am J Roentgenol 155:1251–1255
6. Binkovitz L, Berquist T, McLeod (1990) Masses of the hand and wrist: detection and characterization with MR imaging. AJR Am J Roentgenol 154:323–326
7. Bongartz G, Vestring T, Peters P (1992) Magnetresonanztomographie der Weichteiltumoren. Radiology 32:584–590
8. Capelastegui A, Astigarraga E, Fernandez-Canton G, Saralegui I, Larena JA, Merino A (1999) Masses and pseudomasses of the hand and wrist: MR findings in 134 cases. Skeletal Radiol 28:498–507
9. Cerofolini E, Landi A, Desantis G, Maiorana A, Canossi G, Romagnoli R (1991) MR of benign peripheral nerve sheath tumors. J Comput Assist Tomogr 15:593–597
10. Crim J, Seeger L, Yao L, Chandnani V, Eckardt J (1992) Diagnosis of soft tissue masses with MR imaging: can benign masses be differentiated from malignant ones? Radiology 185:581–586
11. Daldrup H, Shames D, Wendland M, et al (1998) Correlation of dynamic contrast-enhanced MR imaging with histologic tumor grade. AJR Am J Roentgenol 171:941–949
12. De Beuckeleer LH, De Schepper AM, Vandevenne JE, Bloem (2000) MR imaging of clear cell sarcoma (malignant melanoma of the soft parts): a multicenter correlative MRI-pathology study of 21 cases and literature review. Skeletal Radiol 29(4):187–195
13. De Schepper A, Ramon F, Degryse H (1992) Magnetic resonance imaging of soft tissue tumors. J Belge Radiol 75:286–296
14. De Schepper A, Ramon F, Degryse H (1992) Statistical analysis of MRI parameters predicting malignancy in 141 soft tissue masses. Rofo Fortschr Geb Rontgenstr Neuen Bildgeb Verfahr 156:587–591
15. De Schepper A, De Beuckeleer L, Vandevenne J, Somville J (2000) Magnetic resonance imaging of soft tissue tumors. Eur Radiol 10:213–222
16. Elias DA, White LM, Simpson DJ, Kandel RA, Tomlinson G, Bell RS, Wunder JS (2003) Osseous invasion by soft-tissue sarcoma: assessment with MR imaging. Radiology 229(1):145–152
17. Erlemann R, Reiser M, Peters P, Vasallo P, Nommenson B, Kusnierz-Glaz C, Ritter J, Roessner A (1989) Musculoskeletal neoplasms: static and dynamic Gd-DTPA-enhanced MR imaging. Radiology 171:767–773
18. Erlemann R, Sciuk J, Wuisman P, Bene D, Edel G, Ritter J, Peters P (1992) Dynamische MR-Tomographie in der Diagnostik entzündlicher und tumoröser Raumforderungen des musculoskeletalen Systems. Rofo Fortschr Geb Rontgenstr Neuen Bildgeb Verfahr 156:353–359
19. Fleming I (1992) Staging of pediatric cancers. Semin Surg Oncol 8:94–97
20. Fletcher B, Hanna S, Fairclough D, Gronemeyer S (1992) Pediatric musculoskeletal tumors: use of dynamic contrast-enhanced MR imaging to monitor response to chemotherapy. Radiology 184:243–248
21. Galant J, Marti-Bonmati L, Soler R, et al (1998) Grading of subcutaneous soft tissue tumors by means of their relationship with the superficial fascia on MR imaging. Skeletal Radiol 27:657–663
22. Gielen JL, De Schepper AM, Vanhoenacker F, Parizel PM, Wang XL, Sciot R, Weyler J (2004) Accuracy of MRI in characterization of soft tissue tumors and tumor-like lesions. A prospective study in 548 patients. Eur Radiol 14(12):2320–2330
23. Greenfield G, Arrington J, Kudryk B (1993) MRI of soft tissue tumors. Skeletal Radiol 22:77–84
24. Hanna SL, Fletcher B (1995) MR Imaging of malignant soft tissue tumors. Magn Reson Imaging Clin N Am 3:629–650
25. Harkens K, Moore T, Yuh W, Kathol M, Hawes D, El-Khoury G, Berbaum K (1993) Gadolinium-enhanced MRI of soft tissue masses. Australas Radiol 37:30–34
26. Hermann G, Abdelwahab I, Miller T, Klein M, Lewis M (1992) Tumour and tumour-like conditions of the soft tissue: magnetic resonance imaging features differentiating benign form malignant masses. Br J Radiol 65:14–20
27. Kransdorf M (1995) Malignant soft tissue tumors in a large referral population: distribution of specific diagnoses by age, sex and location. AJR Am J Roentgenol 164:129–134
28. Kransdorf M (1995) Benign soft tissue tumors in a large referral population: distribution of specific diagnoses by age, sex and location. AJR Am J Roentgenol 164:395–402
29. Kransdorf M, Murphey M (1997) Imaging of soft tissue tumors. WB Saunders, Philadelphia
30. Kransdorf M, Jelinek J, Moser R (1993) Imaging of soft tissue tumors. Radiol Clin North Am 31:359–372
31. Ma L, Frassica F, Scott E, Fishman E, Zerhouni E (1995) Differentiation of benign and malignant musculoskeletal tumors: potential pitfalls with MR imaging. Radiographics 15:349–366
32. Ma L, Frassica F, McCarthy E, et al (1997) Benign and malignant musculoskeletal masses: MR imaging differentiation with rim-to-center differential enhancement ratios. Radiology 202:739–744
33. Marti-Bonmati L (2004) Benign/malignant classifier of soft tissue tumors using MR imaging. Mag Reson Mater Phys Biol Med 16(4):194–201
34. Meiss-Kindblom J, Enzinger F (1996) Color atlas of soft tissue tumors. Mosby-Wolfe, St Louis
35. Miller T, Potter H, McCormack R (1994) Benign soft tissue masses of the wrist and hand: MRI appearances. Skeletal Radiol 23:327–332
36. Moulton J, Blebea J, Dunco D, Braley S, Bisset G, Emery K (1995) MR imaging of soft tissue masses: diagnostic efficacy and value of distinguishing between benign and malignant lesions. AJR Am J Roentgenol 164:1191–1199
37. Petasnick J, Turner D, Charters J, Gitelis S, Zacharias C (1986) Soft tissue masses of the locomotor system: comparison of MRI with CT. Radiology 160:125–133
38. Sundaram M, McLeod R (1990) MR imaging of tumor and tumorlike lesions of bone and soft tissue. AJR Am J Roentgenol 155:817–824
39. Sundaram M, Sharafuddin M (1995) MR Imaging of benign soft tissue masses. Magn Reson Imaging Clin N Am 3:609–627
40. Sundaram M, McGuire M, Herbold D, Beshany S, Fletcher J (1987) High signal intensity soft tissue masses on T2-weighted pulse sequence. Skeletal Radiol 16:30–34
41. Tacikowska M (2002) Dynamic MR imaging of soft tissue tumors with assessment of the rate and character of lesion enhancement. Med Sci Monit 8(2):MT31–35
42. Tacikowska M (2002) Dynamic magnetic resonance imaging in soft tissue tumors- assessment of the diagnostic value of tumor enhancement rate indices. Med Sci Monit 8(4):MT53–57
43. Totty W, Murphy W, Lee J (1986) Soft tissue tumors: MR imaging. Radiology 160:135–141
44. Tung G, Davis L (1993) The role of magnetic resonance imaging in the evaluation of the soft tissue mass. Crit Rev Diagn Imaging 34:239–308
45. Vanel D, Shapeero L, Tardivon A, et al (1998) Dynamic contrast-enhanced MRI with subtraction of aggressive soft tissue tumors after resection. Skeletal Radiol 27:505–510
46. Van der Woude H, Verstraete K, Hogendoorn P, et al (1998) Musculoskeletal tumors : does fast dynamic contrast-enhanced subtraction MR imaging contribute to the characterization. Radiology 208:821–828
47. van Rijswijk Catharina SP, Geirnaerdt Maarje JA, Hogendoorn Pancras CW, Taminiau Antonie HM, van Coevorden Frits, Zwinderman Aeilko H, Pope Thomas L, Bloem Johan L (2004) Soft-tissue tumors: value of static and dynamic gadopentetae dimeglumine-enhanced MR imaging in prediction of malignancy. Radiology 233:493–502
48. van Unnik JA, Coindre JM, Contesso C, Albus-Lutter CE, Schiodt T, Sylvester R, Thomas D, Bramwell V, Mouridsen HT (1993) Grading of soft tissue sarcomas: experience of the EORTC Sc. Tissue and Bone Sarcoma Group. Eur J Cancer 29A(15):2089–2093
49. Vandevenne J, De Schepper AM, De Beuckeleer L, et al (1997) New Concepts in understanding evolution of desmoid tumors: MR imaging of 30 lesions. Eur Radiol 7:1013–1019
50. Verstraete K (1994) Dynamic contrast-enhanced magnetic resonance imaging of tumor and tumor-like lesions of the musculoskeletal system. Thesis, University of Ghent

51. Verstraete K, De Deene Y, Roels H, Dierick A, Uyttendaele D, Kunnen M (1994) Benign and malignant musculoskeletal lesions: dynamic contrast-enhanced MR imaging – parametric "first-pass" images depict tissue vascularization and perfusion. Radiology 192:835–843
52. Weatherall PT (1995) Benign and malignant masses. MR Imaging differentiation. Magn Reson Imaging Clin N Am 3: 669–694
53. Wetzel L, Levine E (1990) Soft tissue tumors of the foot: value of MR imaging for specific diagnosis. AJR Am J Roentgenol 155:1025–1030
54. Wolf R, Enneking W (1996) The staging and surgery of musculoskeletal neoplasms. Orthop Clin North Am 27:473–481